

Chesca, Boris and John, Daniel and Pollett, Richard and Gaifullin, Marat and Cox, Jonathan and Mellor, Christopher and Savelev, Sergey (2017) Magnetic field tunable vortex diode made of $\text{YBa}_2\text{Cu}_3\text{O}_{7-\delta}$ Josephson junction asymmetrical arrays. *Applied Physics Letters*, 111 (6). 062602. ISSN 0003-6951

Access from the University of Nottingham repository:

http://eprints.nottingham.ac.uk/45527/1/pdf_archiveAPPLABvol_111iss_6062602_1_am.pdf

Copyright and reuse:

The Nottingham ePrints service makes this work by researchers of the University of Nottingham available open access under the following conditions.

This article is made available under the University of Nottingham End User licence and may be reused according to the conditions of the licence. For more details see:
http://eprints.nottingham.ac.uk/end_user_agreement.pdf

A note on versions:

The version presented here may differ from the published version or from the version of record. If you wish to cite this item you are advised to consult the publisher's version. Please see the repository url above for details on accessing the published version and note that access may require a subscription.

For more information, please contact eprints@nottingham.ac.uk

Magnetic field tunable vortex diode made of $\text{YBa}_2\text{Cu}_3\text{O}_{7-\delta}$ Josephson junction asymmetrical arrays

Boris Chesca¹, Daniel John¹, Richard Pollett¹,
Marat Gaifulin¹, Jonathan Cox¹, Christopher Mellor², Sergey Savelev¹

¹Department of Physics, Loughborough University
Loughborough, LE11 3TU, United Kingdom

²School of Physics and Astronomy, University of Nottingham
Nottingham, NG7 2RD, United Kingdom

PACS numbers: 74.78.Na, 73.23.-b, 74.25.Fy

Abstract

Several Josephson ratchets designed as asymmetrically structured parallel-series arrays of Josephson junctions made of $\text{YBa}_2\text{Cu}_3\text{O}_{7-\delta}$ have been fabricated. From the current-voltage characteristics measured for various values of applied magnetic field, B , in the temperature range (10-89) K we demonstrate that the devices work as magnetic field-tunable highly reversible vortex diodes. Thus, at 89 K the ratchet efficiency η could be reversed from +60% to -60% with a change in B as small as $3\mu\text{T}$. By decreasing the operation temperature η improves up to -95% at 10K while the dynamics in the B -tunability degrades. The ratchet designs we propose here can be used to control unidirectional vortex flow vortices in superconducting devices, as well as, building integrated nano-magnetic sensors. Numerical simulations qualitatively confirm our experimental findings and also provide insight into the related and more general problem of the control of the transport of nano/quantum objects in thin films.

Introduction

In the fast developing field of nanoscience the question as to how to control nanoparticle transport on the nanoscale is very important [1-5]. The role of particles drifting in nanodevices can be played not only by tiny bits of materials (say metallic or ferromagnetic spheres) but also by different excitations (quasi-particles), including those of electromagnetic, electronic, and acoustic origin. For example, an applied magnetic field B penetrates a superconductor as an ensemble of magnetic flux quanta Φ_0 , known as vortices [6] whose dynamics can be controlled by applied alternating, direct or even fluctuating electrical currents. Controlling the motion of vortices in superconducting meso- and nanostructures (which are often called fluxtronic devices) has several crucial technological applications. These include the removal of noisy vortices from sensitive parts of superconducting electronics (without the inconvenience of warming-up the devices above the superconducting transition temperature) or creating a specific micro-magnetic profile in mesoscopic superconductors [7]. Purpose-built devices that show a preferential direction of vortex motion are called vortex ratchet devices. Different types of vortex ratchet devices employing meso/nano-scopic superconductors with asymmetric pinning sites have been proposed (see for example Refs. [7-12]) and realized [13-19]. It is important to stress that a significant feature of the fluxtronic devices is their great tuneability as compared to their electronic counterparts, for instance, the vortex diode fabricated and tested in Ref. [13] allows the direction of rectification to be reversed simply by tuning the applied B . Another type of

fluxtronic devices based on utilizing the temporal asymmetry of applied drives to guide magnetic flux quanta [20, 21] has also been successfully implemented [22-24] for both Abrikosov vortices (formed in bulk superconducting materials) and Josephson vortices (trapped in a Josephson junction-*JJ*- formed in a proximity region between two superconductors). Josephson ratchets based on asymmetric current bias configurations have also been fabricated [25-27]. Josephson vortices are very mobile objects and can play a crucial role in both classical and quantum ratchets (see for example Refs. [28-30]), where current reversal effects can be observed at the transition from quantum to classical regimes [28, 31]. Another interesting type of ratchet is based on asymmetric *JJ*-arrays [15, 32] or asymmetric superconducting quantum interferometer devices (SQUIDs) [33-35]. Such ratchets are based on a device's structural/fabrication asymmetry and have the advantage of being more robust against unwanted environmental electromagnetic, electrical, or magnetic interference than other types of ratchets that have been fabricated so far. Indeed, in ratchets based on asymmetric current bias configurations the environmental noise (of electrical/magnetic nature) can interfere destructively with the current bias and decrease its efficiency. Ratchets based on a device's structural/fabrication asymmetry have been recently fabricated and they showed remarkable features such as: a record current amplification at temperatures above 77K [36], a dual flux-to-voltage response [37] and an ability to amplify the self-induced electromagnetic radiation [38]. However, due to their complexity (the design consisted of a parallel-array of 22x20 *JJs* connected by variable areas of SQUID-like holes) such devices have not been simulated numerically, and consequently the physics behind their behaviour could not be fully understood. To achieve a better understanding of such ratchets based on asymmetric *JJ*-structures, in this paper we report the fabrication, measurement and numerical simulation of three less complex designs.

Experimental results

The *JJ*-arrays were fabricated by depositing high quality epitaxial, 100 nm thick *c*-axis oriented YBa₂Cu₃O₇₋₈ (YBCO) films on 10x10 mm², 24° symmetric [001] tilt SrTiO₃ bicrystals by pulsed laser deposition. A 200nm thick Au layer was deposited in situ on top of the YBCO film to facilitate fabrication of high quality electrical contacts for electric transport measurements. The films, with a critical temperature of T_c of 92K, were subsequently patterned by optical lithography and etched by an Ar ion beam to form either a single asymmetric parallel array of 10 *JJs* (see Fig. 1a), 2 (see Fig. 1b), or 9 identical such arrays connected in series (Fig.1c). Within each such parallel array all 10 *JJs* are 3μm wide. The junctions are separated by superconducting loops of identical width of 3μm but variable length. The loops' length increases linearly from 8μm to 16μm in steps of 1μm. Since the individual SQUID inductances, L_n , are proportional to the SQUID loop perimeter (1μm corresponds to approximately 1pH) $\beta_{Ln} = 2\pi L_n I_c / \Phi_0$ also increases monotonically by 58% within the 10 *JJs*-array, with $n=1, 2, \dots, 9$ where I_c is the *JJs* critical current. One can therefore define an average value $\beta = \langle \beta_{Ln} \rangle$ for the array. β can be estimated from both the modulation of I_c with B or direct calculations. At 89 K, we estimated that β_{Ln} varies from 0.27 to 0.54 within the array, while at 10 K it varies from 50 to 100. The bias current I is applied symmetrically via the central top and bottom electrodes and V is measured across the array. B is applied perpendicular to the planar array's structure via a control current I_{ctrl} through an inductively coupled coil. Consequently, an external magnetic flux, Φ_{ex} , is coupled into the array. We fabricated two devices for each of the three designs considered here and for each of the designs both devices showed a qualitatively similar behaviour. Since there is no visible hysteresis in the current-voltage characteristics (*IVCs*) measured, the capacitance of our *JJs*

can be considered to be negligible. Therefore each JJ -array can be modelled as an array of resistively shunted junctions connected via superconducting inductances.

Families of IVC 's were measured by a 4 point-contact method at various temperatures T between 10K and 92K and for different values of I_{ctrl} in the range (-8mA, 8mA). I_{ctrl} was changed in small steps of $15\mu\text{A}$. Such families of consecutive IVC 's measured at different temperatures are plotted in the left hand side insets of Figs. 2 and 3. From such families of IVC 's scanned over I_{ctrl} (or equivalently, B or Φ_{ex}) $V(B)$ for both positive and negative bias currents have been constructed (see Figs. 2, 3 and 4). The corresponding $I_c(B)$ curves look qualitatively similar to the $V(B)$ plots. At temperatures close to T_c , β_{Ln}/π is negligibly small. In this limit $V(\Phi_{ex})$ and $I_c(\Phi_{ex})$ for a symmetrical parallel 10 JJs -array (i.e., an array with identical SQUID holes) should have a periodic pattern consisting of a series of maxima (shown by a dashed line in Fig. 2) similar to the diffraction pattern of a multiple slit optical grating [39]. The flux periodicity corresponds to one additional Φ_0 in each loop. It is remarkable that although the arrays we measured are asymmetric, qualitatively the flux periodicity expected for a symmetric design is still visible to some degree in the experiments carried out at 89K (see Figs. 2 and 4). As expected, with decreasing temperature I_c and the average β_{Ln} both increase and consequently any trace of periodicity in the $V(B)$ vanish quickly (see measurements taken at 10K shown in Fig. 3). From the $V(B)$ curves the ratchet efficiency can be calculated as: $\eta = \left| \frac{V(I)+V(-I)}{V(I)-V(-I)} \right| \times 100\%$. The $\eta(B)$ dependencies for various values of I are shown in Figs. 2, 3 and 4.

To be able to interpret the $\eta(B)$ dependencies one has to first understand the physics involved. When B is applied perpendicularly to a JJ -array plane some flux quanta are trapped in the array loops. I flowing across the array produces a Lorentz force which drives the flux quanta unidirectionally, forming a lattice of vortices moving with a speed, v . This vortex motion produces a dc voltage V across the array which can be measured. In a symmetrical array (i.e. an array with identical array loop areas and junctions) the intensity of the flux flow (and consequently V) is identical for both positive and negative I . As a result, as confirmed by our simulations, $\eta(B)$ is always zero, independent of the value of B (see Fig. 5a). In our experiments, however, for most values of B , $\eta(B)$ is very different from zero with values above 40% at all measured temperatures and reaching almost 100% at 10K for particular values of B . This suggests that the vortex flux flow is highly preferential in one direction, i.e., the device operates as a vortex diode. Moreover, as we change B , $\eta(B)$ changes its sign repeatedly suggesting that the device works as a B -tunable (highly reversible) Josephson vortex diode. Thus at 89K, $\eta(B)$ could be reversed from +60% to -60% (sample B) and from +40% to -40% (sample A) with a change in B as small as $3\mu\text{T}$ (see Fig. 2). The dynamics in the B -tunability is significantly suppressed with decreasing temperature. Thus for a single 10JJ parallel array η switches from positive to negative values 8 times within a $80\mu\text{T}$ range at 89K (see Fig. 2), but it does so only once or twice within a $40\mu\text{T}$ range at 10K (see Fig. 3). Such B -tunability can find application in electronic devices based on multiple JJs such as rapid single flux quantum (RSFQ) [40], SQUIDs [41], or superconducting quantum interference filters (SQIFs) [42, 43] when a tunable preferential direction of flux flow is required. In order to qualitatively understand why efficiency changes sign when B is varied, it is important to understand that usually, during the device's operation, there are many Φ_0 per array loop involved in the ratchet's dynamics. Therefore instead of analysing the vortex motion of all the vortices, one can instead look at the dynamics of flux interstitials only; that is an extra vortex quanta or one missed vortex relative to a perfect matching configuration of integer Φ_0 per array loop at a given applied B . Since the extra Φ_0 and the vortex holes (i.e., a missing vortex) have opposite preferred direction of motion (since they have opposite magnetic

charge') and the transition from an extra vortex dominated picture to a hole dominated picture occurs when magnetic flux varies by one flux quanta per smallest array loop area in the array the efficiency will change sign when B is varied. This is in agreement with our measurements.

Self-induced magnetic fields of the order $L_{average}I$ are generated by the carrying lines. Here $L_{average}=30\text{pH}$ is the average array loop inductance and I is the bias current, typically slightly larger than the Josephson critical current (about $100\mu\text{A}$ at 89K and 18mA at 10K). $L_{average}I$ takes therefore values between $(6 \times 10^{-7}, 3 \times 10^{-9})\mu\text{T}$ as we change temperature in the range $(10, 89)\text{K}$. These values are negligible small relative to a few μT required to significantly modulate $\eta(B)$ (see Figs. 2, 3 and 4). This also suggests that our ratchets are quite robust against unwanted environmental electromagnetic noise which typically will induce currents in the range of nA . Such small currents will be insufficient to produce magnetic fields that will affect the ratchet point of operation.

At 89K , $\eta(B)$ maxima of single parallel 10JJ -arrays (Fig. 1a) are significantly larger (see right-hand side graphs in Fig.2) than a maximum of about 30% reached for a design consisting of 2 such arrays connected in series (Fig.1b) and much larger than about 10% (see inset in Fig. 4) reached for a design consisting of 9 such arrays in series (Fig. 1c). A similar behaviour has been observed at all temperatures in the range $(10-89)\text{K}$: $\eta(B)$ is highest for parallel 10JJ -arrays, is significantly lower for 2 serially-connected 10JJ -arrays, and is smallest for the 9 serially-connected 10JJ -arrays. These observations suggest that when N parallel-arrays are connected in series the ratchet efficiency decreases rapidly with N . This effect can be easily understood if considering the spread of I_c of the individual JJ -arrays connected [41]. Indeed, since the resulting voltage of N parallel 10JJ -arrays connected in series is the sum of all individual voltages for all bias currents taking values in the range (minimum I_c , maximum I_c) some 10JJ -arrays will be in the voltage state showing some ratchet efficiency and some will be in the zero-voltage state showing no ratchet efficiency. Consequently the overall effect on the entire device's ratchet efficiency will be diluted when connecting N parallel 10JJ -arrays in series relative to a single 10JJ -array.

Theoretical model and simulations

The design asymmetry of the JJ -arrays can be implemented in three different ways using the asymmetry in the Josephson critical currents of n th junction j_{cn} or/and in the array loop areas A_n : (i) symmetric j_{cn} and asymmetric A_n ; (ii) asymmetric j_{cn} and symmetric A_n ; (iii) asymmetric j_{cn} and A_n ; Simulations show (see Fig. 5a) that in order to maximise efficiency η the best way to implement asymmetry is by keeping j_{cn} of all junctions the same and varying A_n (symmetric j_{cn} and asymmetric A_n). It is for this reason that this case has been realized in practice.

The asymmetric Josephson transmission line can be described by a set of coupled ordinary differential equations [44]:

$$\begin{aligned} \frac{d\varphi_0}{dt} &= j - j_{c0}(1 + \Delta_J)\sin\varphi_0 + \alpha \left[\frac{\varphi_1 - \varphi_0}{(1 + \Delta_A)A_{\frac{1}{2}}} - h \right] + \sqrt{2D} \xi_0 \\ \frac{d\varphi_n}{dt} &= j - j_{cn}(1 + \Delta_J)\sin\varphi_n + \alpha \left[\frac{\varphi_{n+1} - \varphi_n}{(1 + \Delta_A)A_{n+\frac{1}{2}}} - \frac{\varphi_n - \varphi_{n-1}}{(1 + \Delta_A)A_{n-\frac{1}{2}}} \right] + \sqrt{2D} \xi_n \\ \frac{d\varphi_{n_{max}}}{dt} &= j - j_{cn_{max}}(1 + \Delta_J)\sin\varphi_{n_{max}} + \alpha \left[h - \frac{\varphi_{n_{max}} - \varphi_{n_{max}-1}}{(1 + \Delta_A)A_{n_{max}-\frac{1}{2}}} \right] + \sqrt{2D} \xi_{n_{max}}. \end{aligned}$$

(1)

In order to match the experimentally implemented design, n runs from 1 to 8 in the middle equation of set (1), while $n_{\max} = 9$ in the last equation of the set. We denote the dimensionless applied current $j = I/\langle I_c \rangle$, with $\langle I_c \rangle$ being the array's average I_c , φ_n (with $n=0, \dots, 9$) is the gauge invariant phase difference across the n th junction, dimensionless time t is measured in the units of the characteristic relaxation time $\tau = \Phi_0/2\pi cRI_c$ with the flux quantum Φ_0 , the speed of light c , and the junction resistance R (assumed the same for all junctions). The detailed consideration of two dimensional boundary conditions of the problem suggests the same j in all junctions of the line. We also introduce parameter $\alpha = \tau cR/(4\pi aS_{1/2})$ with the inter-junction distance a and the smallest area $S_{1/2}$ of the array loop between junctions with $n=0$ and $n=1$. The array loop area linearly increases with junction number and area ratio $A_{n+1/2} = S_{n+1/2}/S_{1/2} = 1+n/8$, with $n+1/2$ refers to the array loop between n th and $(n+1)$ th junctions. The dimensionless magnetic flux $h = HS_{1/2}/\Phi_0$, is measured in units of magnetic flux quantum per smallest array loop area of the array. In the simulations we also considered the effect of two types of structural fluctuations related to the JJ -arrays: (i) critical current fluctuations from junction to junction Δ_j , with the average $\langle \Delta_j \rangle = 0$, i.e., I_{cn} of the n th junction can vary randomly from the designed value (due to inhomogeneities of the bicrystal line [41]) resulting in fluctuations of $j_{cn} = I_{cn}/\langle I_c \rangle$; (ii) fluctuations in the array loop areas Δ_A , with the average $\langle \Delta_A \rangle = 0$, due to the $1 \mu\text{m}$ finite resolution of photolithography used in the fabrication process. Finally, thermal fluctuations have been considered too: temporal unbiased δ -correlations Gaussian white noise ξ_n with intensity D , i.e., $\langle \xi_n \rangle = 0$, $\langle \xi_n(0)\xi_n(t) \rangle = \delta(t)$, which can occur, for instance, due to thermal noise or temporal current fluctuations of the external circuit. In order to estimate η we average the time derivative of the gauge invariant phase difference over time and junctions $\bar{\varphi}(j) = \langle \langle d\varphi_n/dt \rangle_n \rangle_t$ and use the dimensionless ratchet efficiency, $\eta = \left| \frac{\bar{\varphi}(j) + \bar{\varphi}(-j)}{\bar{\varphi}(j) - \bar{\varphi}(-j)} \right| \times 100\%$. The effect on η of all these three types of fluctuations is shown in Fig. 5b. It is important to notice that while large thermal fluctuations ($D > 0.5$) or critical current fluctuations significantly suppress η , moderate fluctuations in the array loop areas ($\langle \Delta_A^2 \rangle^{1/2}$ in the range (0, 0.5)) have an insignificant effect on η . The corresponding experimental points (indicated by vertical arrows) are shown in the insets of Fig. 5b.

To compare the simulation results with the experimental data, we consider $\eta(B)$ at a fixed value of I . The red curve in Fig. 6 represents results without structural fluctuations ($\Delta_j = 0$ and $\Delta_A = 0$) and temporal noise $D = 0$. In this case, it is possible to show that any solution of Eqs. (1) should be periodic as a function of h with period $\Delta h = 16\pi$, which is clearly seen in the upper inset of Fig. 6 (red curve). Spatial fluctuations of I_{cn} eliminate such fragile periodicity (upper inset in Fig. 6, blue curve), making it very difficult to observe experimentally (no experimental evidence has been found in our data). In order to make a qualitative comparison with the experiment results we plot an enlarged part of the upper inset in the main panel of Fig. 6. Comparing the simulated result with, say, experimental data shown in Figs. 2, 3 and 4, we conclude that the model captures the main experimental features well: the order of magnitude of the ratchet effect, the variation of η with B and the change of rectification directions (reversible rectification tuned by B). Comparing the simulated rectification with and without spatial fluctuations of the critical current, we also expect that each sample (where such fluctuations are unavoidable and uncontrollable) should have its individual fingerprint, thus requiring individual calibration for practical usage. Also, the presence of the Earth's magnetic field B_E generates a shift in the magnetic field axis, resulting in some additional uncertainty for quantitative comparison of experimental data and

simulations. The amount of flux coupled into the array due to B_E is also difficult to estimate considering the well-know large flux focusing effects in bicrystal Josephson junctions [41, 42]. For these reasons, here we restrict ourselves with only a qualitative comparison between the model and the experimental data and this indicates good agreement between them.

Taking advantage of the ability to explore a large temperature range in detail within our simulations, we vary temperature from very low values to T_c at fixed values for I and B . $\eta(T)$ is shown in the lower inset of Fig. 6. In contrast to the quite unpredictable dependence of $\eta(B)$ (Fig. 6), $\eta(T)$ exhibits a clear peak (lower inset of Fig. 6) when the applied current reaches the critical current of the sample $j = j_{cn}(T_{sw})$ (or its minimum value if j_{cn} fluctuates) that occurs at a certain well-defined temperature, T_{sw} . This could be used to design a temperature switch which changes its state when the temperature crosses the value, $T_{sw}(h)$. Importantly, the switching temperature can be tuned by the applied B . This effect is robust with respect to a certain amount of white noise (lower inset of Fig. 6) which further justifies the potential of the discussed effect for temperature switching applications.

Conclusions

The operation of magnetically tunable Josephson ratchets designed as asymmetrically structured parallel or parallel-series JJ arrays made of $\text{YBa}_2\text{Cu}_3\text{O}_{7-\delta}$ has been demonstrated in a wide temperature range (10-89)K. The ratchet efficiency η could be very efficiently controlled by B : at 10K η drops from -95% to 0% when B changes by 12 μ T (see Fig. 3), while at 89K η could be reversed from +60% to -60% (in sample B) or from +40% to -40% (sample A) with a change in B as small as 3 μ T (see Fig. 2). Arrays connected in parallel have a significantly improved ratchet efficiency η in comparison to parallel-series arrays. Such vortex diodes are excellent potential candidates in applications where controlling unidirectional vortex flow is essential such as SQUIDs, SQIFs, or RSFQ.

References

- [1] P. Hanggi and F. Marchesoni, *Rev. Mod. Phys.* 81, 387 (2009).
- [2] P. Hanggi, F. Marchesoni, and F. Nori, *Ann. Phys.* 14, 51 (2005).
- [3] S. Savel'ev and F. Nori, *Chaos* 15, 026112 (2005).
- [4] C. Bustamante, J. Liphardt, and F. Ritort, *Physics Today* 58, 43 (2005).
- [5] J. Huguet, C. V. Bizarro, N. Forns, S. B. Smith, C. Bustamante, and F. Ritort, *PNAS* 107, 15431 (2010).
- [6] M. Tinkham, *Introduction to Superconductivity* (Dover Publications Inc.; 2nd Revised edition edition, 2004).
- [7] C.S. Lee, B. Janko, I. Derenyi, and A.L. Barabasi, *Nature* 400, 337 (1999).
- [8] J. F. Wambaugh, C. Reichhardt, C.J. Olson, F. Marchesoni, and F. Nori, *Phys. Rev. Lett.* 83, 5106 (1999).
- [9] C.J. Olson, C. Reichhardt, B. Janko, and F. Nori, *Phys. Rev. Lett.* 87, 177002 (2001).
- [10] S. Savel'ev, F. Marchesoni, and F. Nori, *Phys. Rev. Lett.* 91, 010601 (2003).
- [11] S. Savel'ev, F. Marchesoni, and F. Nori, *Phys. Rev. Lett.* 92, 160602 (2004).
- [12] S. Savel'ev, F. Marchesoni, and F. Nori, *Phys. Rev. E* 70, 061107 (2004).
- [13] J. E. Villegas, Sergey Savel'ev, Franco Nori, E. M. Gonzalez, J. V. Anguita, R. García, and J. L. Vicent, *Science* 302, 1188 (2003).
- [14] J. B. Majer, J. Peguiron, M. Grifoni, M. Tusveld, and J.E. Mooij, *Phys. Rev. Lett.* 90, 056802 (2003).
- [15] D. E. Shalom and H. Pastoriza, *Phys. Rev. Lett.* 94, 177001 (2005).
- [16] M. Beck, E. Goldobin, M. Neuhaus, M. Siegel, R. Kleiner, and D. Koelle, *Phys. Rev. Lett.* 95, 090603 (2005).

- [17] J. Van de Vondel, C. C. de Souza Silva, B. Y. Zhu, M. Morelle, and V. V. Moshchalkov, *Phys. Rev. Lett.* **94**, 057003 (2005).
- [18] Y. Togawa, K. Harada, T. Akashi, H. Kasai, T. Matsuda, F. Nori, A. Maeda, and A. Tonomura, *Phys. Rev. Lett.* **95**, 087002 (2005).
- [19] C. C. de Souza Silva, J. Van de Vondel, M. Morelle and V. V. Moshchalkov, *Nature* (London) **440**, 651 (2006).
- [20] S. Savel'ev and F. Nori, *Nature Mater.* **1**, 179 (2002).
- [21] S. Savel'ev, F. Marchesoni, P. Hanggi, and F. Nori, *Europhys. Lett.* **67**, 179 (2004); *Eur. Phys. J. B* **40**, 403 (2004).
- [22] D. Cole, S. Bending, S. Savel'ev, A. Grigorenko, T. Tamegai, and F. Nori, *Nature Mater.* **5**, 305 (2006).
- [23] S. Ooi, S. Savel'ev, M. B. Gaifullin, T. Mochiku, K. Hirata, and F. Nori, *Phys. Rev. Lett.* **99**, 207003 (2007).
- [24] A. V. Ustinov, C. Coqui, A. Kemp, Y. Zolotaryuk, and M. Salerno, *Phys. Rev. Lett.* **93**, 087001 (2004).
- [25] R. Gerdemann, T. Bauch, O.M. Froehlich, L. Alff, A. Beck, D. Koelle, and R. Gross, *Appl. Phys. Lett.* **67**, 1010 (1995).
- [26] J. Schuler, S. Weiss, T. Bauch, A. Marx, D. Koelle, and R. Gross, *Appl. Phys. Lett.* **78**, 1095 (2001).
- [27] T. Bauch, S. Weis, H. Haensel, A. Marx, D. Koelle, and R. Gross, *IEEE Trans. Appl. Supercond.* **7**, 3605 (1997).
- [28] A. O. Sboychakov, S. Savelev, A. L. Rakhmanov, and F. Nori, *Phys. Rev. Lett.* **104**, 190602 (2010).
- [29] S. Savelev, A.L. Rakhmanov, and F. Nori, *Phys. Rev. Lett.* **98**, 077002 (2007).
- [30] S. Butz, A.K. Feofanov, K.G. Fedorov, H. Rotzinger, A.U. Thomann, B. Mackrodt, R. Dolata, V.B. Geshkenbein, G. Blatter, and A.V. Ustinov, *Phys. Rev. Lett.* **113**, 247005 (2014).
- [31] P. Reimann, M. Grifoni, and P. Hanggi, *Phys. Rev. Lett.* **79**, 10 (1997).
- [32] V. I. Marconi, *Phys. Rev. Lett.* **98**, 047006 (2007).
- [33] I. Zapata, R. Bartussek, F. Sols, and P. Hanggi, *Phys. Rev. Lett.* **77**, 2292 (1996).
- [34] I. Zapata, J. Luczka, F. Sols, and P. Hanggi, *Phys. Rev. Lett.* **80**, 829 (1998).
- [35] F. Falo, P. J. Martinez, J.J. Mazo, and S. Cilla, *Europhys. Lett.*, **45**, 700 (1999).
- [36] B. Chesca, D. John, M. Kemp, J. Brown and C.J. Mellor, *Appl. Phys. Lett.* **103**, 092601 (2013).
- [37] B. Chesca, D. John, and C.J. Mellor, *Supercond. Sci. Technol.* **27**, 055019 (2014).
- [38] B. Chesca, D. John, and C.J. Mellor, *Supercond. Sci. Technol.* **27**, 085015 (2014).
- [39] J. H. Miller, G. H. Gunaratne, J. Huang, and T. D. Golding, *Appl. Phys. Lett.* **59**, 3330-3332 (1991).
- [40] K. K. Likharev, V.K. Semenov, *IEEE Trans. Appl. Supercond.*, **1**, 3, (1991); P. Bunyk, K. K. Likharev, D. Zinoviev, *Int. J. Hi. Spe. Ele. Syst.* **11**, 257 (2001).
- [41] B. Chesca, D. John and C.J. Mellor, *Appl. Phys. Lett.* **107**, 162602 (2015).
- [42] P. Caputo, J. Oppenländer, Ch. Häussler, J. Tomes, A. Friesch, T. Träuble and N. Schopohl, *Appl. Phys. Lett.* **85**, 1389 (2004);
- [43] E. E. Mitchell, K.E. Hannam, J.Y. Lazar, K.E. Leslie, A. Grancea, S.T. Keenan, S. K. H. Lam, and C. P. Foley, *Supercond. Sci. Technol.* **29**, 06LT01 (2016).
- [44] N.F. Pedersen and A.V. Ustinov, *Supercond. Sci. Technol.* **8**, 389 (1995).

Figure Caption

Fig. 1. Optical micrographs showing three devices consisting of (a) a single parallel array of 10 Josephson junctions, (b) 2 and (c) 9 such identical parallel arrays connected in series. The bicrystal grain boundary (GB) is shown by the dotted line in (a). The Josephson junctions are formed across the GB and can be seen as bridges, grey in colour, crossing the GB. Within each parallel array the rectangular holes separating the junctions have an identical width of 3 μm and increasing lengths from 8 to 16 μm ;

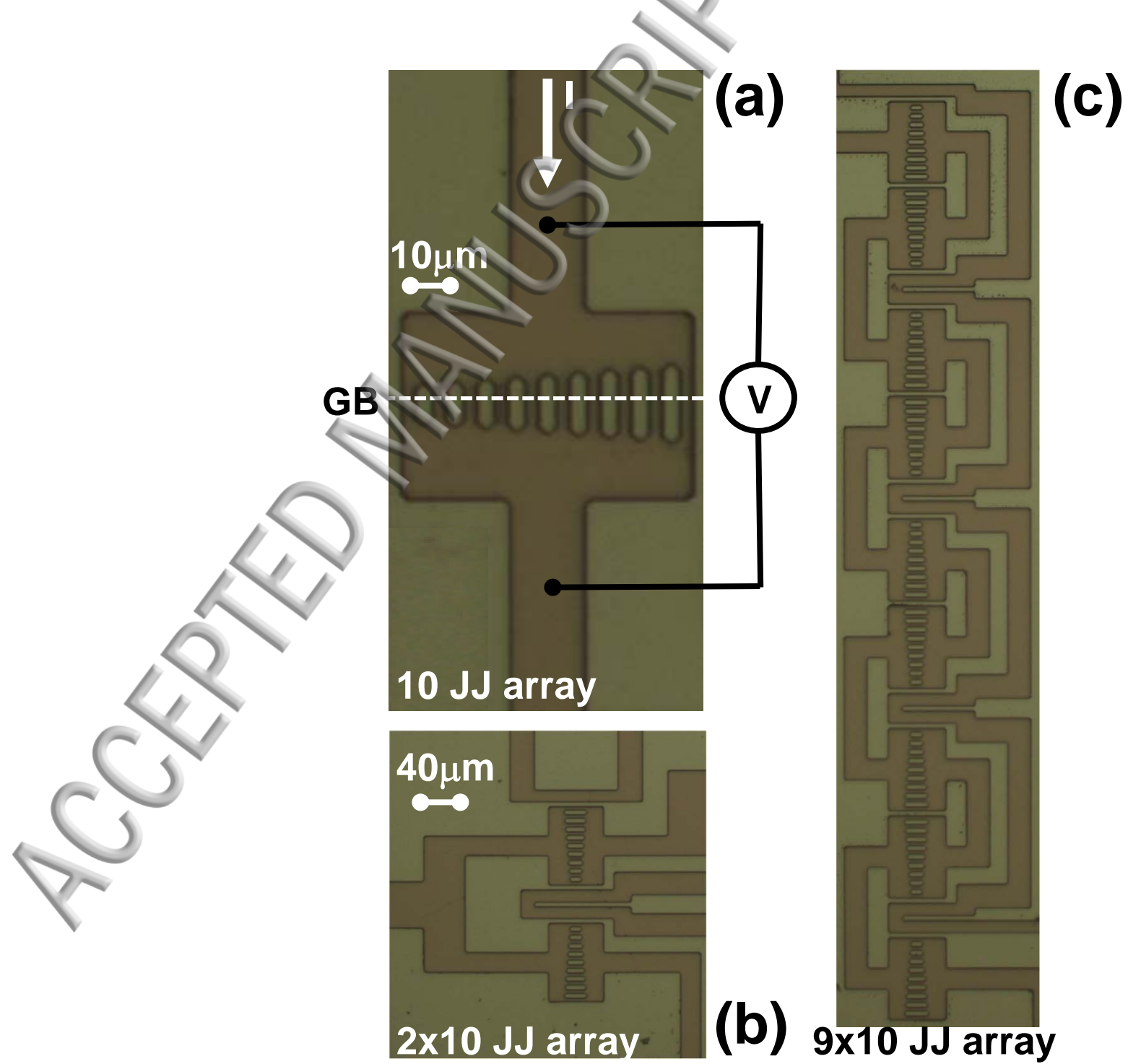
Fig. 2. Electrical transport properties of parallel 10JJ-arrays at 89K (samples A and B). On the left-hand side $V(B)$ is shown for two different values of the bias current, I . The $V(B)$ characteristics were obtained from families of IVC 's taken at multiple B field values (shown in the insets: a single IVC and 221 IVC s). With dashed line in (a) the periodical theoretical curve of $V(B)$ is shown calculated using the approach developed in [39]. From $V(B)$ the ratchet efficiency $\eta(\%)$ has been calculated (right-hand side figures).

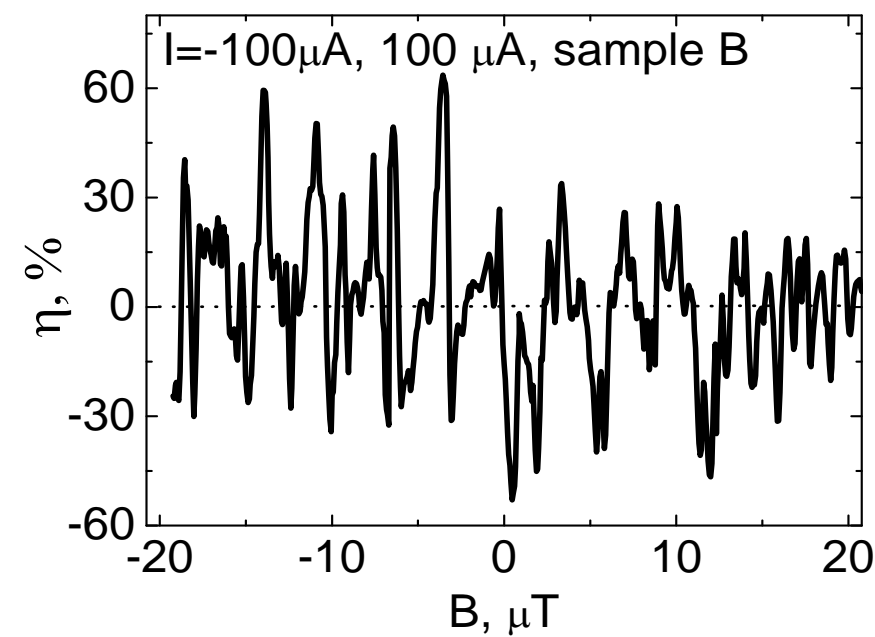
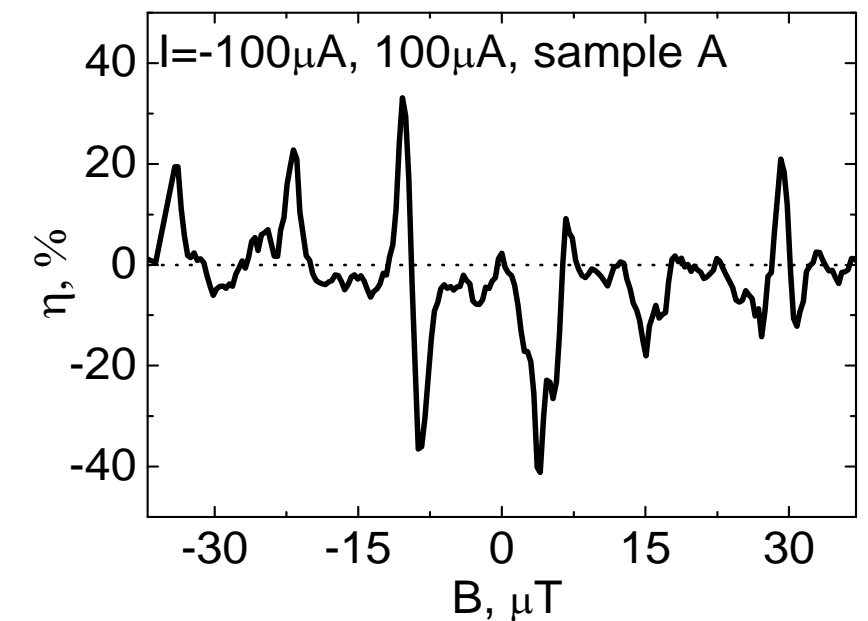
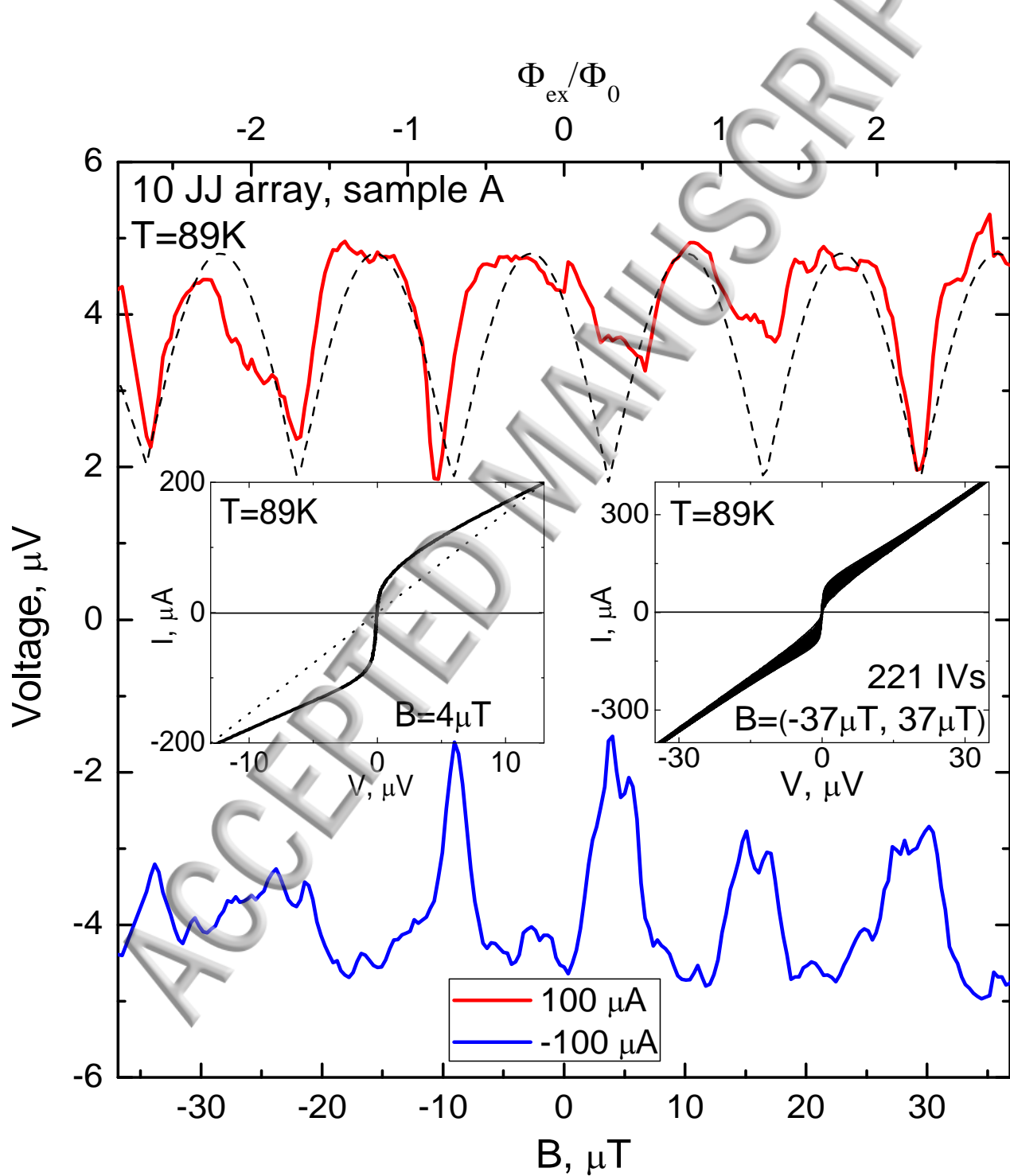
Fig. 3. Electrical transport properties of a parallel 10JJ-array at 10K (sample A). On the left-hand side $V(B)$ is shown for two different values of the bias current, I . The $V(B)$ characteristics were obtained from families of IVC 's taken at multiple B field values. From $V(B)$ the ratchet efficiency $\eta(\%)$ has been calculated (right-hand side figures).

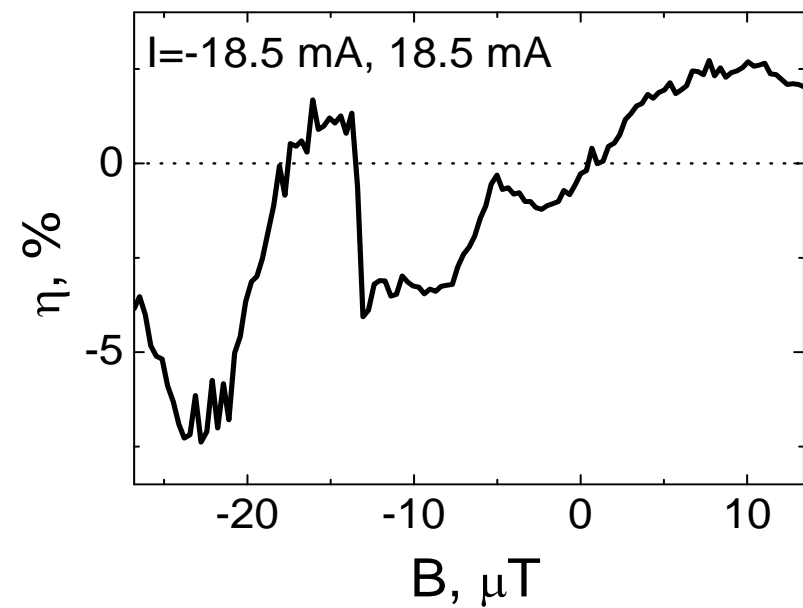
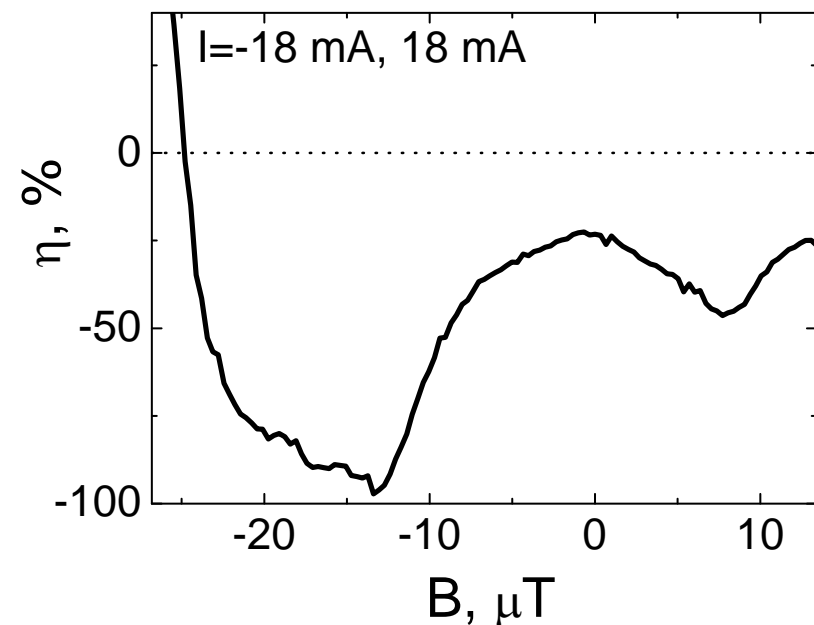
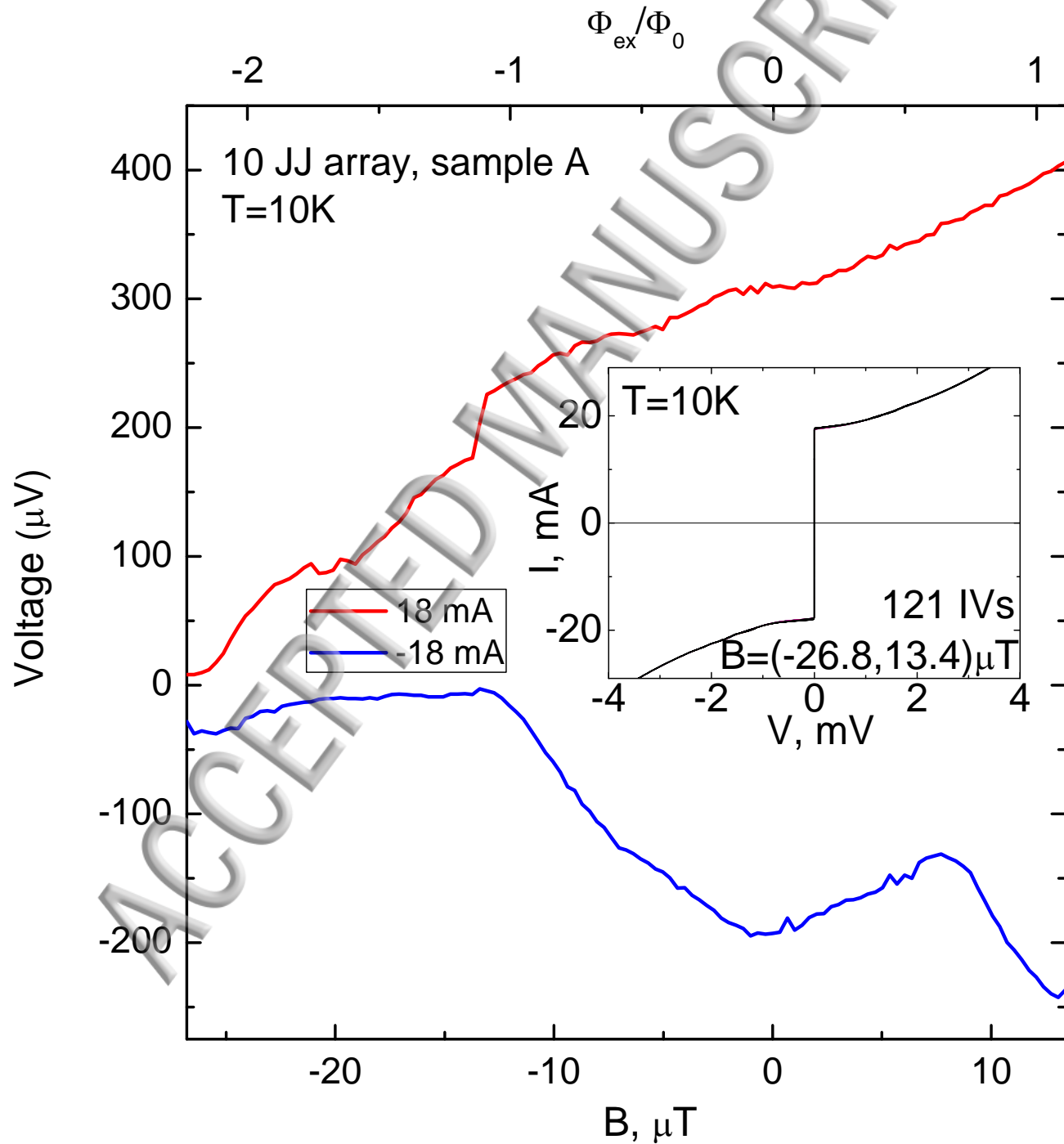
Fig. 4. Electrical transport properties at $T=89\text{K}$ of a parallel-series device consisting of nine 10JJ parallel arrays connected in series. $V(B)$ is shown for two different values of the bias current, I . From $V(B)$ the ratchet efficiency $\eta(\%)$ has been calculated (right-hand side figures).

Fig. 5. (a) $\eta(\%)$ versus B for three possible ways of ratchet asymmetry implementation: symmetric j_{cn} and asymmetric A_n (top-left design); asymmetric j_{cn} and symmetric A_n (bottom-right design); asymmetric j_{cn} and A_n ; the case of symmetric j_{cn} and A_n when no ratchet effect is observed is shown too; (b) The effect of fluctuations on η calculated for a ratchet with symmetric j_{cn} and asymmetric A_n and a bias current of 10% above the Josephson critical current. Three types of fluctuations are considered: thermal noise, J_c fluctuations (lower inset), and fluctuations in the array loop area (upper inset).

Fig. 6. Electrical transport properties simulated by using Eq. (1). The ratchet efficiency $\eta(h) = \left| \frac{\bar{\varphi}(j,h) + \bar{\varphi}(-j,h)}{\bar{\varphi}(j,h) - \bar{\varphi}(-j,h)} \right|$ as a function of the applied magnetic field h for applied current $j=1$, $\alpha = 0.1$, $D=0$, $j_n^c = 1$ (for all n for red curve) and one realization of random j_n^c , which is homogeneously distributed in the interval $[0.5, 1.5]$ (for blue curve). The curves in the upper inset are the same as in the main panel but for larger magnetic field range where periodicity is clearly seen for (red) but not for the blue curve. Lower inset: the temperature dependence of the ratchet efficiency $\eta(T) = \left| \frac{\bar{\varphi}(j,T) + \bar{\varphi}(-j,T)}{\bar{\varphi}(j,T) - \bar{\varphi}(-j,T)} \right|$ for $h=1$, $\alpha = 0.1$; no temporal noise is included in the curves reaching 100% efficiency (i.e., $D=0$): $j_n^c = (1 - T/T_c)$ (for all n); and the applied current $j=0.9$ (red curve), $j=0.5$ (blue curve), and $j=0.3$ (green curve). The ratchet efficiency for $h=1$, $\alpha = 0.1$, $j_n^c = (1 - T/T_c)$, and $j=0.5$ in the presence of temporal noise ($D=D_0T/T_c$, $D_0=0.05$), shown again in blue, is drastically reduced to about 25% in accordance to typical values observed in the experiments at high temperatures.

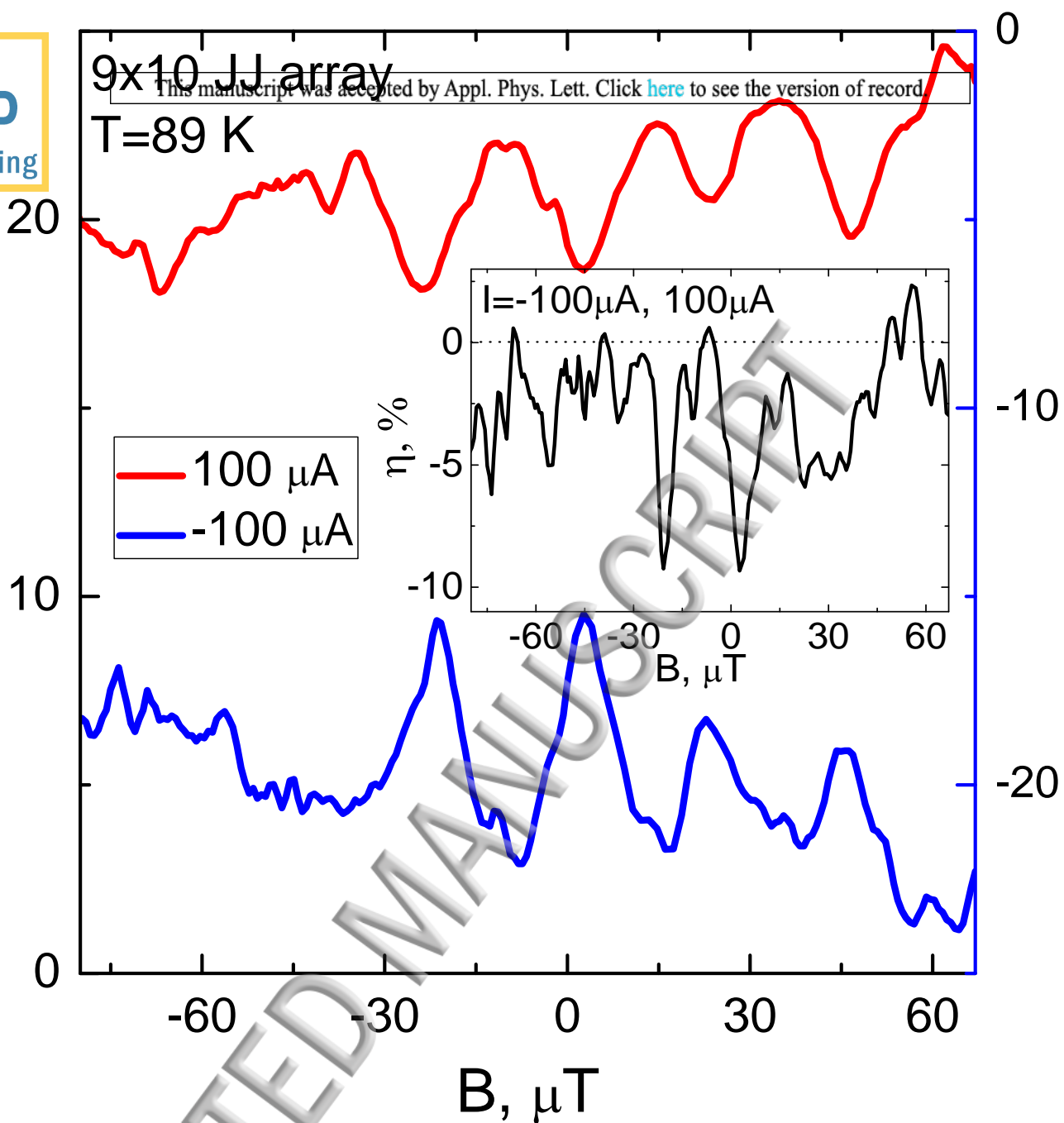






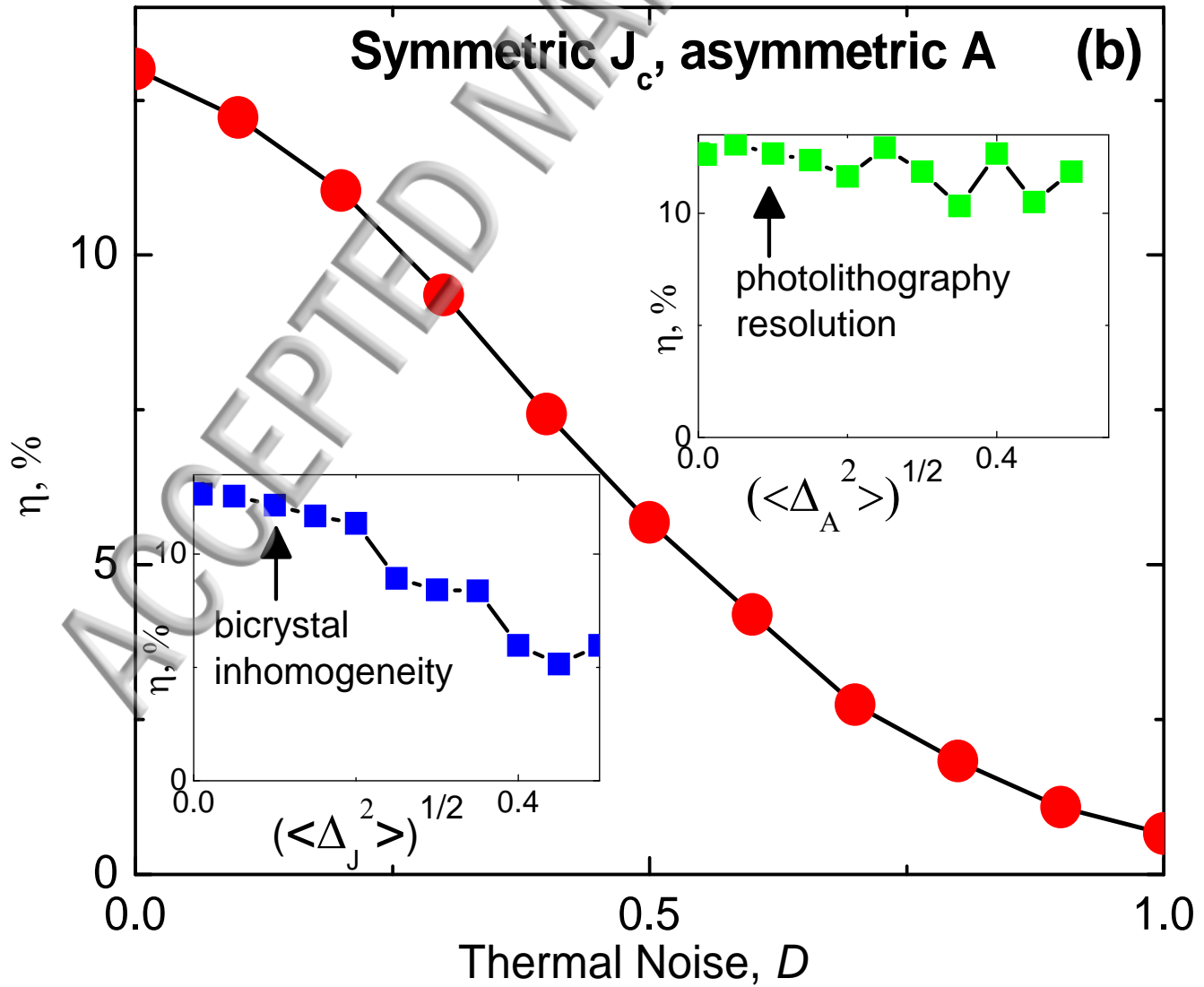
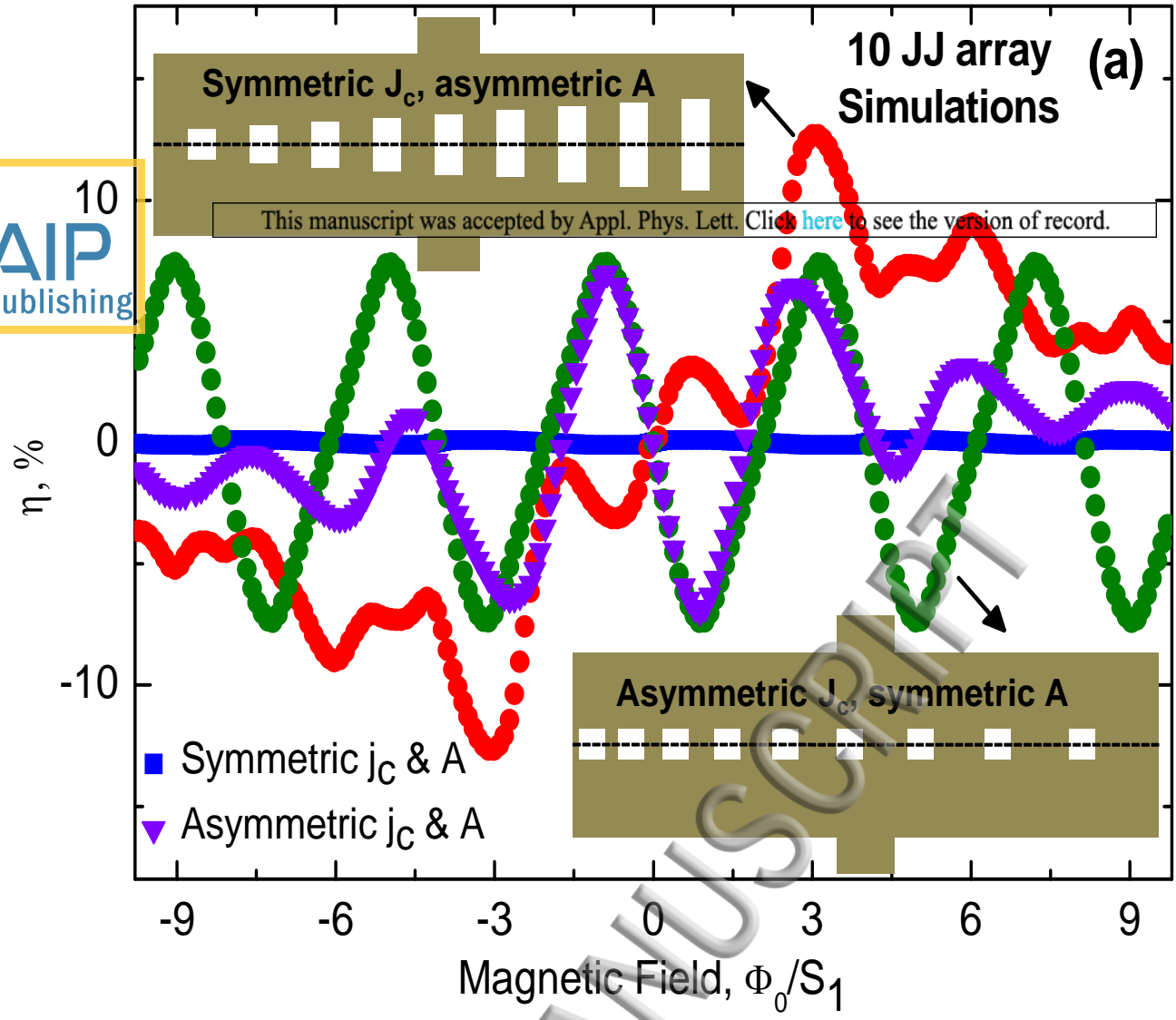
9x10 JJ array
 This manuscript was accepted by Appl. Phys. Lett. Click [here](#) to see the version of record
 T=89 K

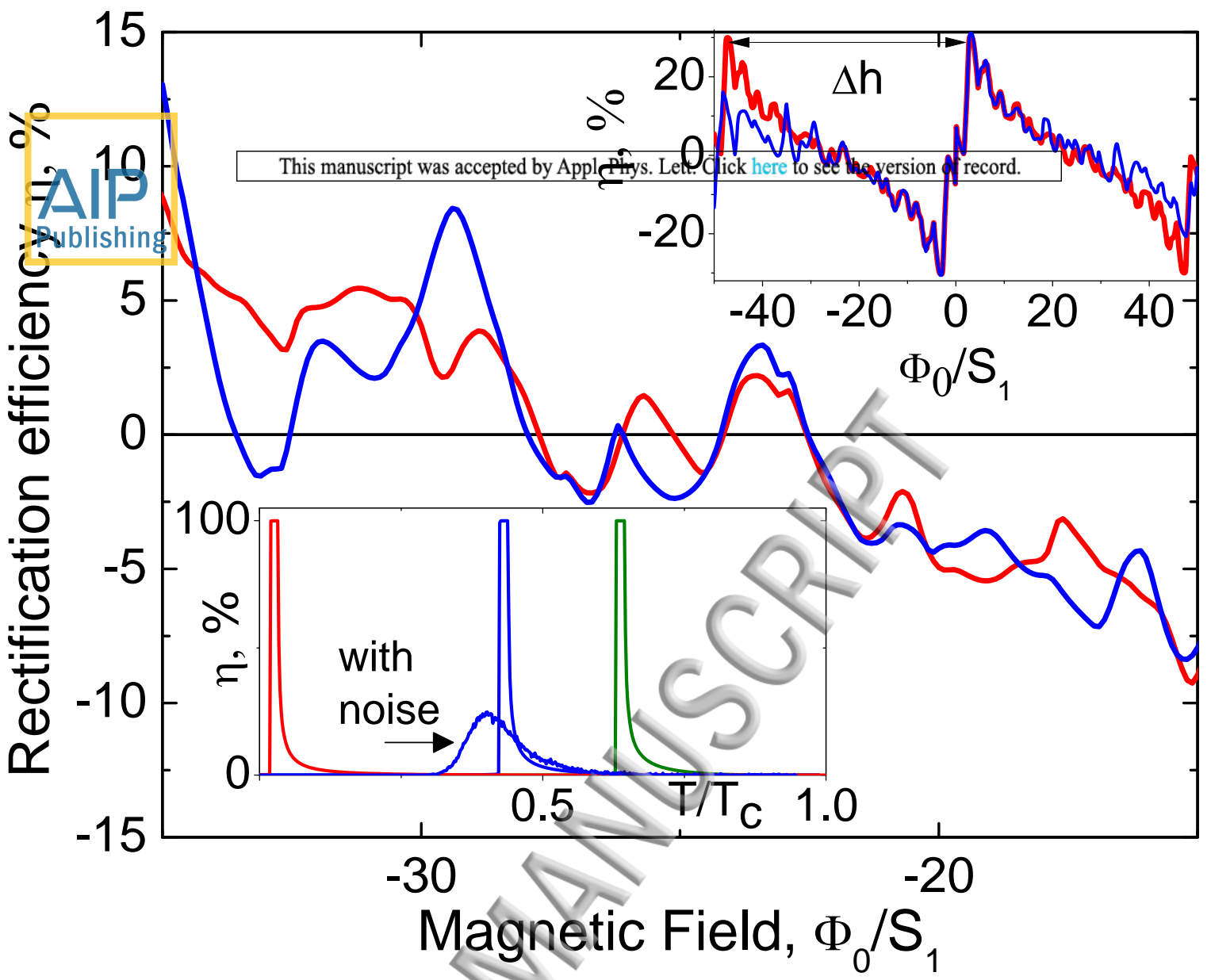
Voltage, μV



Voltage, μV

ACCEPTED MANUSCRIPT





ACCEPTED MANUSCRIPT